Supporting Information

Controlling TiO_2 photocatalytic behavior via perhydropolysilazane-derived SiO_2 ultrathin shell

Darya Burak[a,b], Jae Hyun Han[a,c], Joon Soo Han[a], In Soo Kim[d], Md Abdur Rahman[f], Joel K. W. Yang[f], and So-Hye Cho[a,b*]

[a]Materials Architecturing Research Center, Korea Institute of Science and Technology, 5 Hwarang-ro 14-gil, Seoul 02792, Korea

[b]Division of Nano & Information Technology, University of Science and Technology, 217 Gajeong-ro Yuseong-gu, Daejeon 34113, Korea

[c]Display and Nanosystem Laboratory, College of Engineering, Korea University, Anam-ro 145, Seoul 02841, Republic of Korea

[d]Nanophotonics Research Center, Korea Institute of Science and Technology, 5 Hwarang-ro 14-gil, Seoul 02792, Korea

[f]Engineering Product Development Pillar, Singapore University of Technology and Design, 8 Somapah Road, Singapore 487372, Singapore

Figure S1. Camera-captured images of the PHPS solution (a) after UV-C and (b) UV-A irradiation.

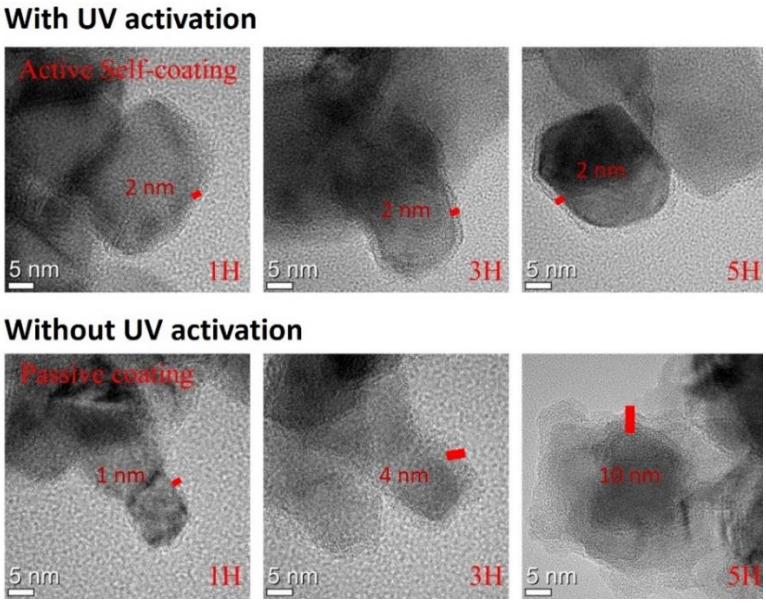

Figure S2. HRTEM images of the TiO_2@PHPS core-shell nanoparticles prepared under UV-irradiated (top) and non-irradiated (bottom) conditions.

Impact of UV irradiation time on formation of PHPS-derived SiO_2 shell. This experiment was conducted in order to determine the optimal duration of UV-A irradiation needed to form a uniform PHPS-derived SiO_2 shell, whereupon the irradiation time was varied from 1, 3 to 5 h. Firstly, the crystalline phases of the nanoparticles were examined, and the results are presented in Figure S3 and S4. The XRD pattern of the anatase TiO_2 nanoparticles exhibited characteristic diffraction peaks[1,2] native to P25 TiO_2. Interestingly, the presence of SiO_2 shells had a discernible impact of the XRD patterns of both TiO_2@TEOS and TiO_2@PHPS core-shell nanoparticles, resulting in broad humps spanning from 20^0 to 40^0.[3]

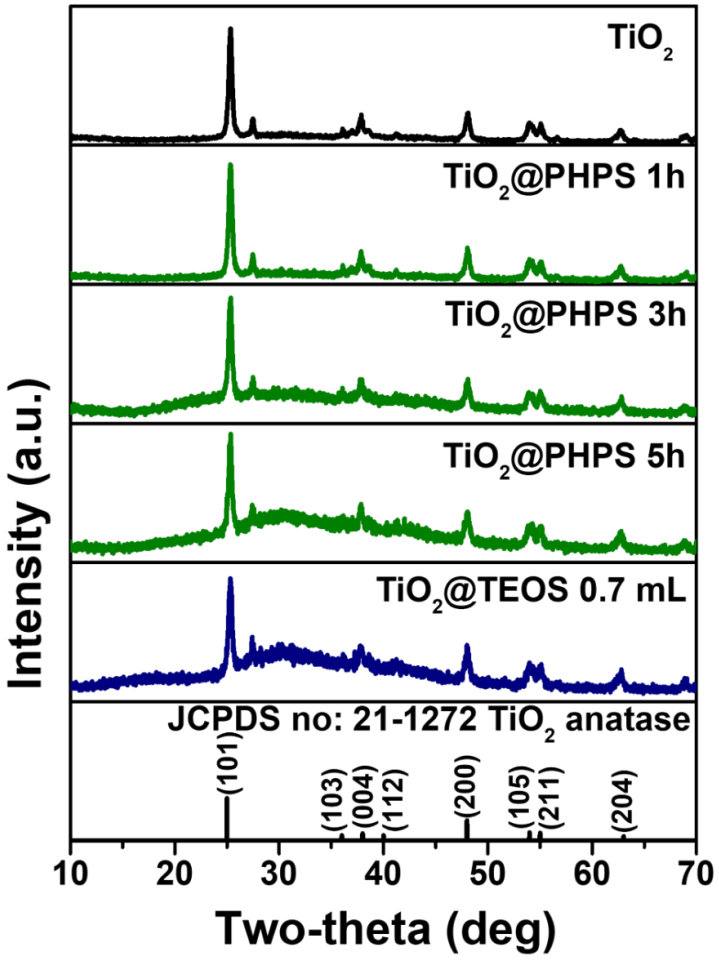

Figure S3. XRD patterns of the TiO_2, TiO_2@TEOS and TiO_2@PHPS core-shell nanoparticles. The TiO_2@PHPS nanoparticles were synthesized under UV-A irradiation time of 1, 3, and 5 h.

[1] K. Wang, Y. Zhuo, J. Chen, D. Gao, Y. Ren, C. Wang, Z. Qi, *RSC Adv.* 2020, **10**, 43592.
[2] V. Mishra, M. K. Warshi, A. Sati, A. Kumar, V. Mishra, R. Kumar, P. R. Sagdeo, *SN Appl. Sci.* 2019, **1**, 241.
[3] S. Nabih, A. E. Shalan, E. S. A. Serea, M. A. Goda, M. F. Sanad, *J. Mater. Sci.: Mater. Electron.* 2019, **30**, 9623–9633.

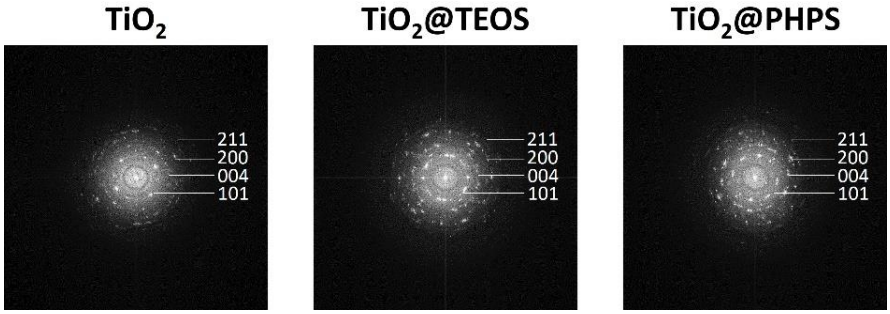

Figure S4. SAED patterns of the TiO_2, TiO_2@TEOS and TiO_2@PHPS core-shell nanoparticles.

FT-IR spectra of the TiO_2@PHPS core-shell nanoparticles synthesized under UV-A irradiation time of 1, 3, and 5 h are shown in Figure S5. Spectra of the bare TiO_2 and TiO_2@TEOS nanoparticles are also presented for comparison. Initially, we ascertained that using 1 mL of PHPS and 0.7 mL of TEOS would yield comparable SiO_2 shell thicknesses, prompting their selection for this experiment (Figure 3b,d). The FT-IR spectra revealed an intense peak at 400 cm^{-1}, corresponding to the stretching vibration of the Ti−O−Ti bond.[4] For the TiO_2@SiO_2 nanoparticles, newly emerged peaks at 1216, 1073 and 936 cm^{-1} were observed. The peak at 1216 cm^{-1} signified the presence of Si−OH groups, while the peaks at 1073 and 936 cm^{-1} resulted from the stretching vibrations of the Si−O−Si and Ti−O−Si bonds, respectively.[5,36,40] Furthermore, for the TiO_2@PHPS nanoparticles, the intensity of the Si−O−Si bond peak notably increased in those prepared after 3-h irradiation, with a modest increment observed in the case of 5-h irradiated nanoparticles. Consequently, these findings suggest an anticipated increase in SiO_2 shell thickness from 1 to 3 h of irradiation for the TiO_2@PHPS particles. However, limited changes in the SiO_2 amount were expected between 3- and 5-h irradiation, indicating that a 3-h irradiation time is sufficient to obtain a PHPS-derived SiO_2 shell. On the other hand, a substantial increase in the intensity of the Si−O−Si bond peak when contrasted with the predominant Ti−O−Ti bond peak in the case of the TiO_2@TEOS nanoparticles suggested that the TEOS-derived SiO_2 shell would be thicker in comparison to the PHPS-derived SiO_2 shells.

[4] V. Etacheri, C. Di Valentin, J. Schneider, D. Bahnemann, S. C. Pillai, *J. Photochem. Photobiol. C: Photochem. Rev.* 2015, **25**, 1–29.

[5] J. Guo, S. Yuan, Y. Yu, J. R. van Ommen, H. V. Bui, B. Liang, *RSC Adv.* 2017, **7**, 4547.

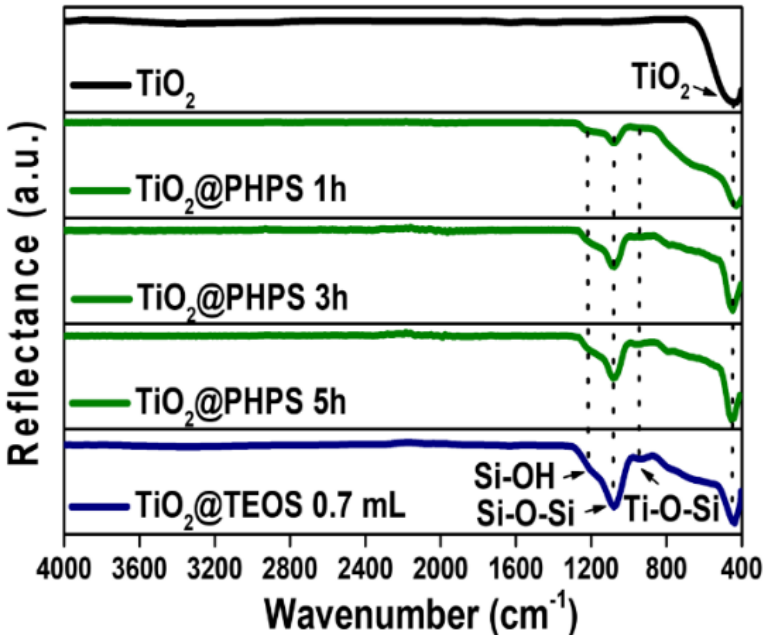

Figure S5. FT-IR spectra of the TiO_2, TiO_2@TEOS, and TiO_2@PHPS core-shell nanoparticles. The TiO_2@PHPS nanoparticles were synthesized under UV-A irradiation time of 1, 3, and 5 h.

Next, the morphologies of TiO_2, TiO_2@TEOS and TiO_2@PHPS nanoparticles were investigated via TEM analysis (Figure S6). The TiO_2@PHPS nanoparticles exposed to 1-h UV-A irradiation exhibited an incomplete SiO_2 shell formation around the TiO_2 core, leaving exposed TiO_2 regions (Figure S6a(ii)). Since the core-shell structure remained incomplete after the 1-h irradiation, it was reasonable to anticipate a lower photocatalytic passivation ability for this sample. Conversely, with 3-h irradiation, a continuous shell coating without evident agglomeration of the SiO_2 nanoparticles was observed (Figure S6a(iii)). Similarly, the 5-h irradiated sample also resulted in a continuous shell coating, comparable to the 3-h irradiated sample, but with some agglomeration, as explained in Figure S7. As for the TiO_2@TEOS nanoparticles, the SiO_2 shell also appeared uniform without noticeable agglomeration, forming TiO_2@SiO_2 core-shell nanoparticles visibly similar to the 3- and 5-h irradiated TiO_2@PHPS particles.

HRTEM measurements were also conducted to further investigate the thickness uniformity of the core-shell nanoparticles (Figure S7). In the case of the 1-h irradiated TiO_2@PHPS nanoparticles, the SiO_2 shell exhibited non-uniform thickness, ranging from 1 to 2 nm. In contrast, consistent with our expectations from FT-IR measurements, there was no significant variation in thickness observed for 3- and 5-h irradiated samples. Although, in the case of the 5-h irradiated sample, a SiO_2 agglomeration occurred around the TiO_2 core nanoparticles, suggesting that extending the irradiation time from 3 to 5 h seemed to transition from an active coating process to a passive one, as PHPS slowly and continuously hydrolyzed in the presence of an aqueous environment in the irradiation system.[3] This process eventually resulted in the excessive formation of SiO_2 nanoparticles and the observed agglomeration. To ensure a consistent comparison of shell thicknesses, we selected an area from HRTEM images that exhibited no agglomeration of SiO_2 nanoparticles (otherwise occurring when the extensive 5-h irradiation led from active to passive SiO_2 formation) for the 5-h irradiated sample. The average thickness remained at 2 nm, indicating a satisfactorily uniform and conformal coating, particularly for the 3-h irradiated sample. This observation led us to conclude that a 3-h irradiation time was sufficient

to fully convert PHPS into SiO_2 via the OH^- photocatalytic sites of TiO_2, resulting in a uniform shell around the TiO_2 core with no undesired SiO_2 particle agglomeration.

On the other hand, the TiO_2@TEOS nanoparticles displayed a noticeable deviation in thickness, with some regions having a thickness of ~2 nm and others reaching as high as ~4 nm, as clearly observed from the HRTEM image (Figure S7). This observation underscored that while TEOS can provide continuous and effective shells,[20-24] achieving a high level of thickness uniformity remains challenging. Since the formation of the SiO_2 shell from TEOS is a passive process, it leads to non-selective deposition around the TiO_2 core. As a result, this can cause aggregation and variations in the shell thickness.

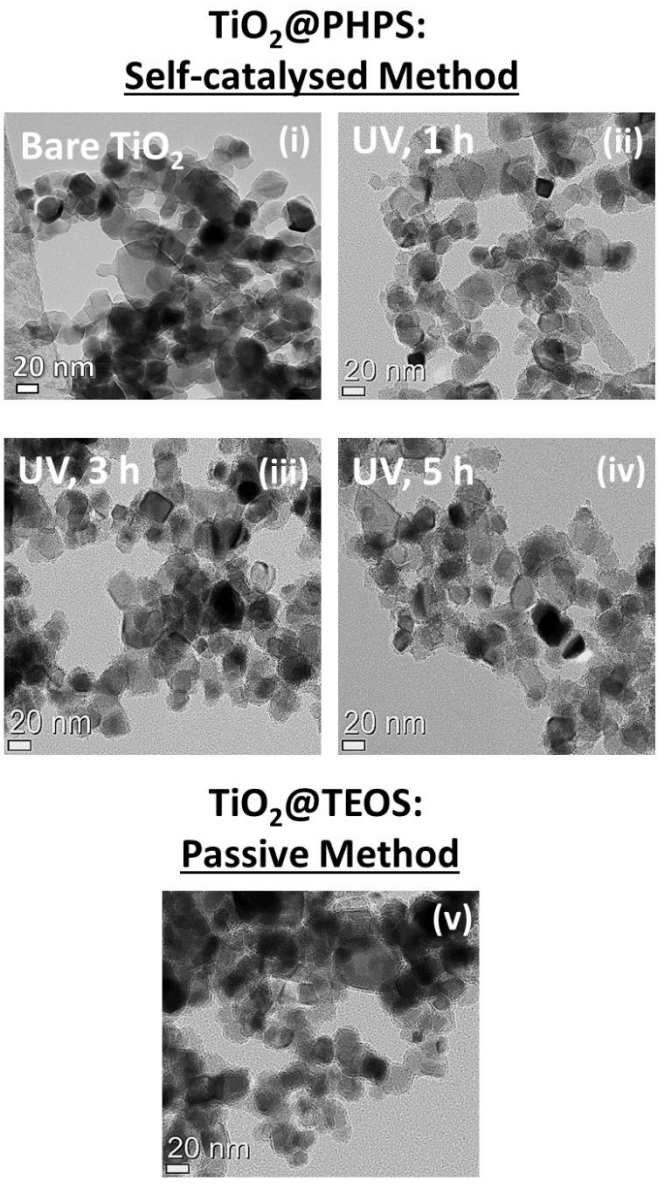

Figure S6. TEM images of the (i) TiO_2, (ii-iv) TiO_2@PHPS core-shell nanoparticles prepared via self-catalysed method, and (v) TiO_2@TEOS core-shell nanoparticles prepared via passive method. The TiO_2@PHPS nanoparticles were synthesized under UV-A irradiation time of 1, 3, and 5 h.

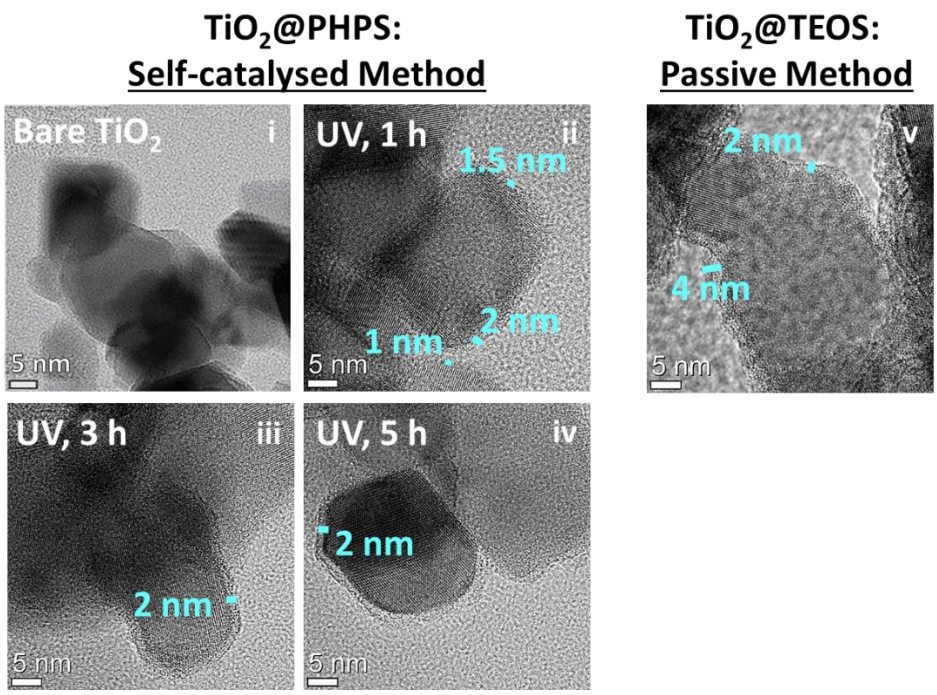

Figure S7. High-resolution TEM images of the bare TiO_2, TiO_2@TEOS and TiO_2@PHPS core-shell nanoparticles prepared via self-catalysed and passive methods, respectively. The TiO_2@PHPS nanoparticles were synthesized under UV-A irradiation time of 1, 3, and 5 h.

The passivation of TiO_2 photocatalytic activity was assessed by observing the degradation of Eosin B under UV irradiation. Figure S8 demonstrates the photocatalytic performance of the bare TiO_2, TiO_2@TEOS and TiO_2@PHPS core-shell nanoparticles. Upon the exposure to UV irradiation, the concentration of Eosin B decayed rapidly for the uncoated TiO_2, and Eosin B was almost completely consumed within 60 min. A similar effect was observed for the TiO_2@TEOS nanoparticles, which exhibited a significantly greater degradation of Eosin B compared to the TiO_2@PHPS nanoparticles. In the case of the TEOS-derived nanoparticles, the concentration of Eosin B was consumed by marginal 90% after 180 min of UV exposure. On the other hand, for the TiO_2@PHPS nanoparticles, except for the 1-h irradiated sample, where the insufficient thickness and exposed TiO_2 surface areas resulted in a steady decrease in Eosin B concentration, the decay rate was much slower for the 3- and 5-h irradiated samples, indicating a notable passivation of TiO_2 photocatalytic activity.

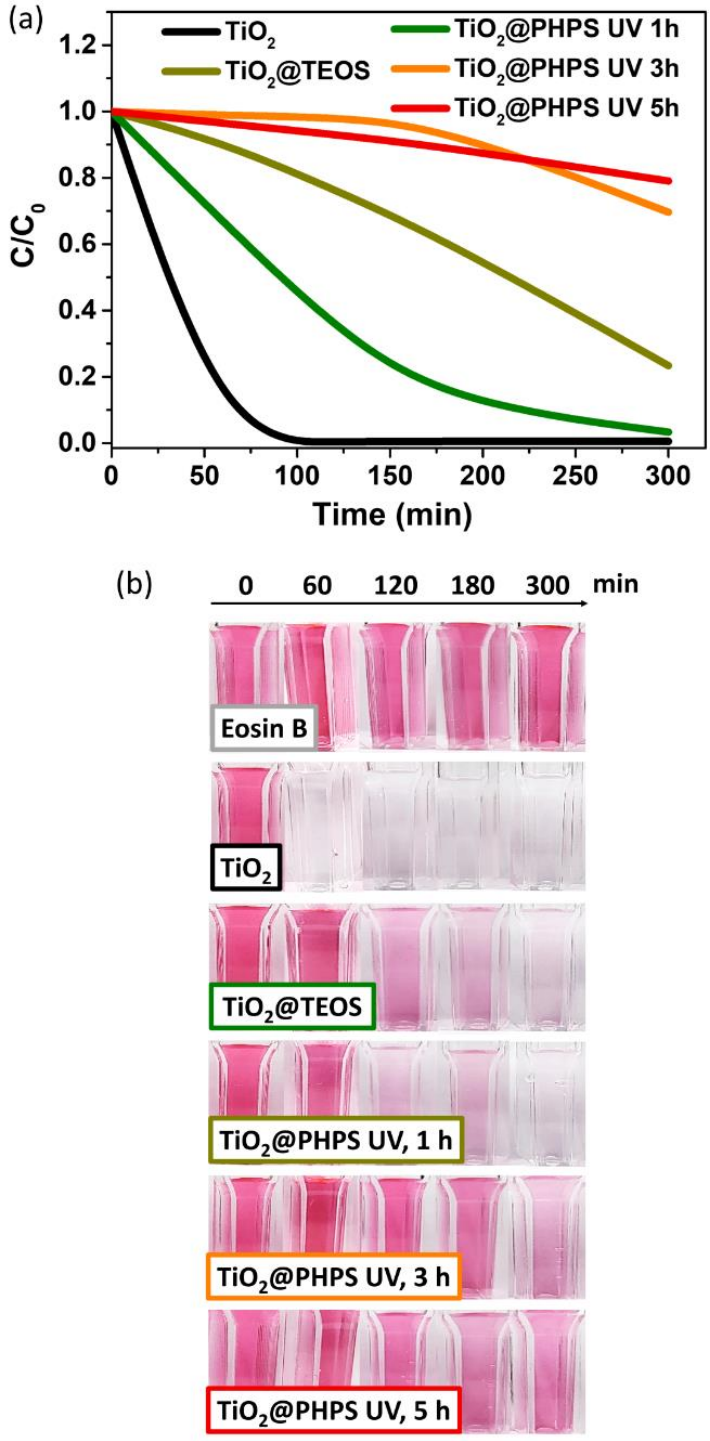

Figure S8. (a) Photocatalytic degradation of Eosin B as a function of time by the TiO_2, 0.7 mL TiO_2@TEOS and 1, 3, and 5-h irradiated TiO_2@PHPS core-shell nanoparticles. (b) Camera-captured images of the Eosin B solution following its photocatalytic degradation by the TiO_2, TiO_2@TEOS and TiO_2@PHPS core-shell nanoparticles under UV irradiation. The TiO_2@PHPS nanoparticles were synthesized under UV-A irradiation time of 1, 3, and 5 h.

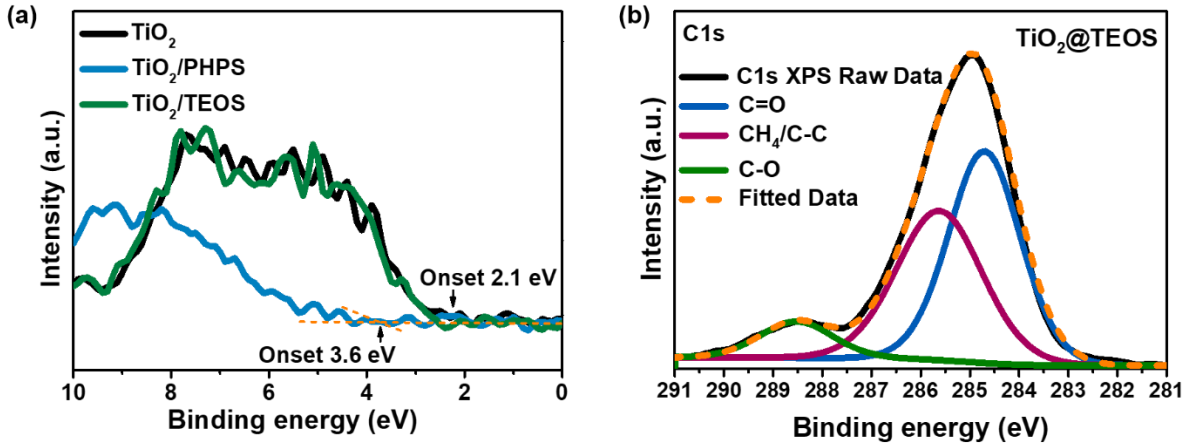

Figure S9. (a) Valence-band XPS spectra of TiO_2, TiO_2/TEOS, and TiO_2/PHPS films. (b) Narrow scan deconvoluted XPS spectrum of C1s binding energy range of the 0.7 mL TiO_2@TEOS.

The deconvoluted narrow scan spectrum of C1s of TiO_2@TEOS nanoparticles revealed three carbon components at 288.5, 285.7, and 284.7 eV. Since TEOS is an organic carbon-containing compound, these observed peaks were assigned to C=O, C−H, and C−C/CH_x bonds, respectively.[2,14]

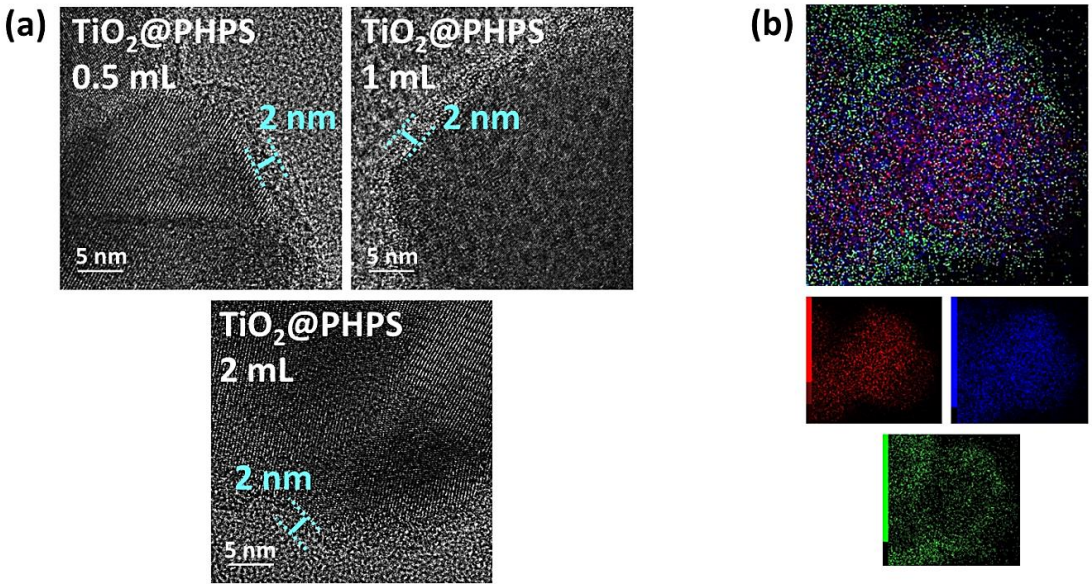

Figure S10. (a) HRTEM images of 0.5, 1, and 2 mL TiO_2@PHPS core-shell nanoparticles, and (b) element mapping of Ti, Si, and O for the 1 mL TiO_2@SiO_2 nanoparticles. (Captured at a higher magnification of 5 nm, compared to the 10 nm magnification used in Figure 3d.)

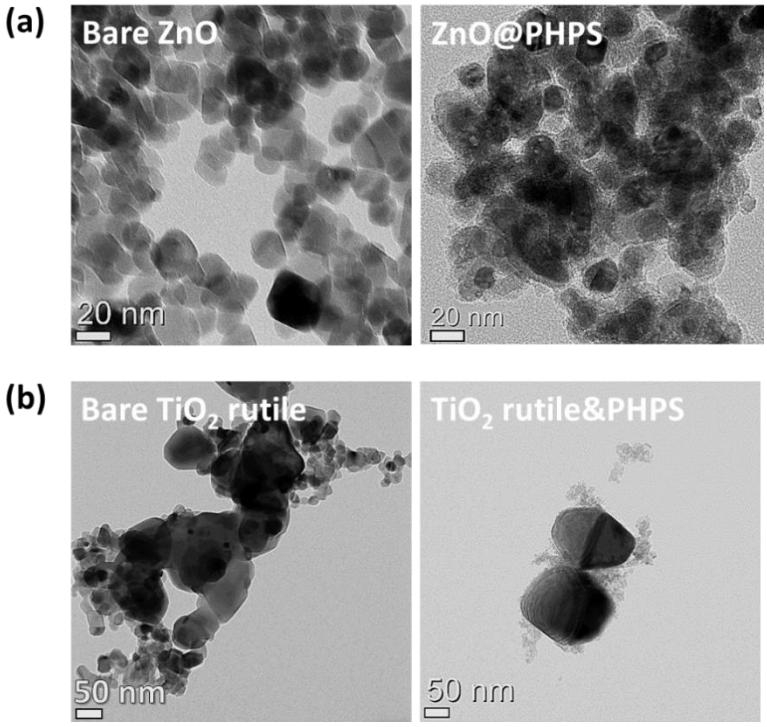

Figure S11. TEM images of the (a) bare ZnO and ZnO@PHPS, and (b) bare TiO_2 rutile and TiO_2 rutile@PHPS core-shell nanoparticles prepared via self-catalysed method.

Table S1. Colour characterization of TiO_2, TiO_2@TEOS, and TiO_2@PHPS nanoparticles based on the CIELAB (L*a*b*) and CMYK (cyan, magenta, yellow, black "key") colour models. The classified parameters based on the CIELAB model are as follows: L* (lightness), a* (+a*: redness, -a*: greenness), b* (+b*: yellowness, -b*: blueness) (exported from SpectraMagic NX Color Data Software [30]). Colour HEX codes [*Nix Sensor Ltd, Free Color Converter*, https://www.nixsensor.com/free-color-converter (accessed 2023-12-05)] were derived from the L*, a*, and b* values. Colour names, their descriptions and corresponding CMYK percentage of colour were obtained from the colour information inferred from [*Color Hexa, Color Encyclopedia: Information and Conversion*, https://www.colorhexa.com (accessed: 2023-12-05)]. TiO_2@PHPS nanoparticles were synthesized by varying the PHPS precursor solution concentration across 0.5, 1, to 2 mL. TiO_2@TEOS nanoparticles were synthesized by varying the TEOS precursor concentration across 0.7, 1, to 1.4 mL.

Sample	Colour parameters			HEX (#)	Colour	Colour description	CMYK Percentage of Colour			
	L*	a*	b*				C	M	Y	K
TiO_2	89.0	-0.62	-0.08	E2E4E4		Light grayish cyan	1%	0%	0%	11%
TiO_2@PHPS 0.5 mL	91.2	-0.62	0.28	E8E9E9		Light grayish cyan	0%	0%	0%	9%
TiO_2@PHPS 1 mL	90.0	-0.62	0.49	E5E6E5		Light grayish lime green	0%	0%	0%	10%
TiO_2@PHPS 2 mL	86.3	-0.62	0.7	DCDDDB		Light grayish green	0%	0%	1%	13%
TiO_2@TEOS 0.7 mL	86.5	-2.02	-2.69	D7DEE2		Light grayish blue	5%	2%	0%	11%
TiO_2@TEOS 1 mL	83.3	-2.89	-1.94	CFD8DA		Light grayish cyan	5%	1%	0%	15%
TiO_2@TEOS 1.4 mL	83.7	-1.13	-2.94	D1D6DA		Light grayish blue	4%	2%	0%	15%

While the L* value of bare TiO_2 was 89.0, it decreased to 86.5, 83.3, and 83.7 for the TiO_2@TEOS nanoparticles with 0.7, 1, and 1.4 mL of TEOS, respectively. Conversely, with the exception of the 2 mL-synthesized TiO_2@PHPS nanoparticles, the remaining samples demonstrated increased L* values. Moreover, the a*b* parameters of all TiO_2@PHPS nanoparticles were closer to 0 compared to those of the TiO_2@TEOS nanoparticles. The following suggested that the PHPS-derived nanoparticles maintained the high whiteness properties of the original TiO_2.

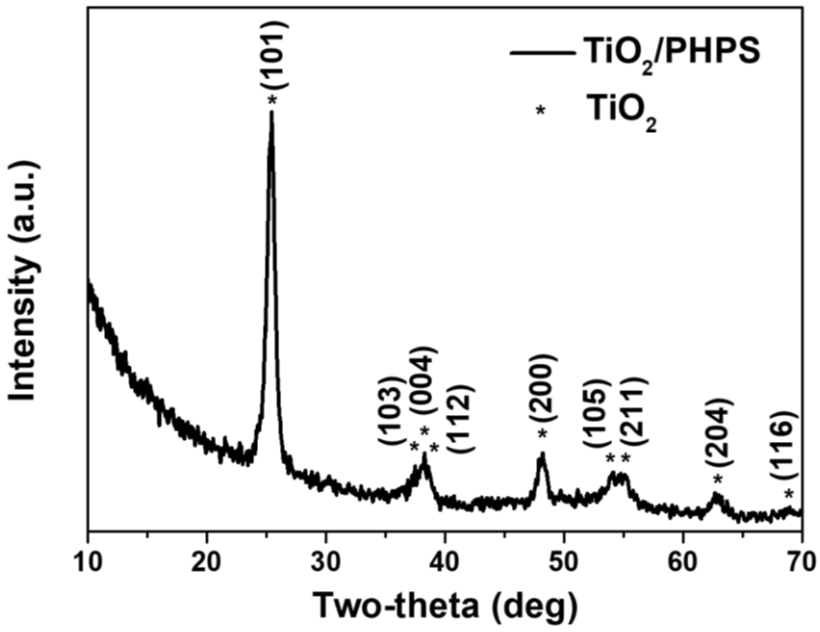

Figure S12. GIXRD patterns of TiO_2 and TiO_2/PHPS films.

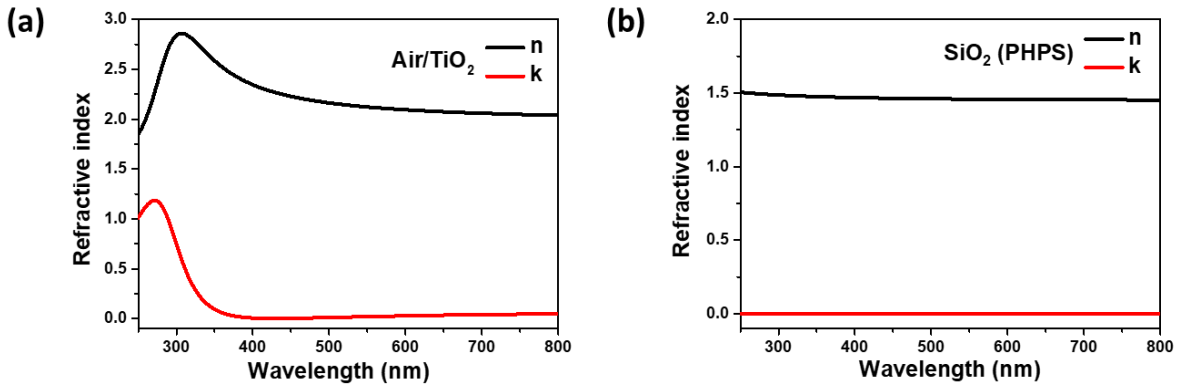

Figure S13. Ellipsometry-measured refractive indices of (a) TiO_2 film and (b) PHPS-derived SiO_2 layer.

Table S2. Colour characterization of TiO_2 and TiO_2/PHPS films based on the CIELAB (L*a*b*) colour model. The classified parameters are as follows: L* (lightness), a* (+a*: redness, -a*: greenness), b* (+b*: yellowness, -b*: blueness) (exported from SpectraMagic NX Colour Data Software [30]. Color HEX codes [*Nix Sensor Ltd, Free Color Converter*, https://www.nixsensor.com/free-color-converter (accessed 2023-12-05)] were derived from the L*, a*, and b* values. Colour names and their descriptions were obtained from the colour information inferred from [*Color Hexa, Color Encyclopedia: Information and Conversion*, https://www.colorhexa.com (accessed: 2023-12-05)].

Sample	Colour parameters			HEX (#)	Colour	Colour description
	L*	a*	b*			
TiO_2	29.81	9.61	-41.08	#2E4387		Dark moderate blue
TiO_2/PHPS	32.79	6.12	-39.27	#304C8C		Dark moderate blue

Table S3. Pencil hardness and cross-cut adhesion test results of TiO_2 and TiO_2/PHPS films.

Sample	Pencil hardness (10H=best)	Cross-cut adhesion (5B=best)
TiO_2	4H	5B
TiO_2/PHPS	4H	5B

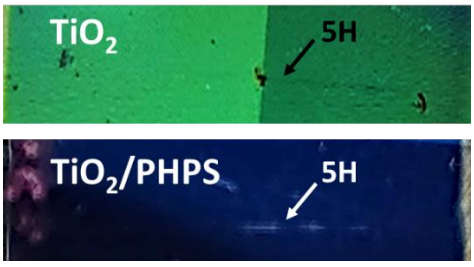

Figure S14. Camera-captured images of TiO_2 and TiO_2/PHPS films after the pencil hardness test. The images exhibit no apparent surface scratches until a 5H hardness pencil was utilized.

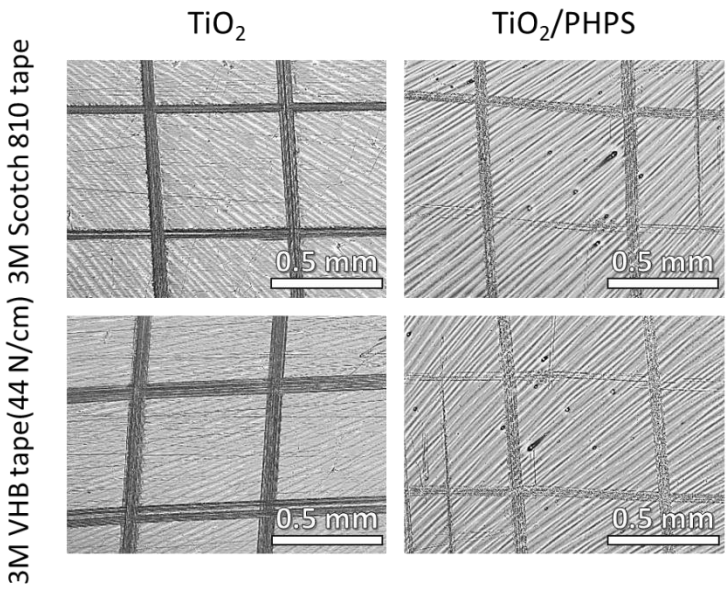

Figure S15. Microscopic images of TiO_2 and TiO_2/PHPS films after the cross-cut adhesion test. Weakly adhesive scotch (3M Scotch 810 tape) and strongly adhesive (3M VHB tape (44 N/cm)) tapes were applied and peeled off vertically in a repeated manner (up to 10 times) to investigate the surface delamination.

The hardness of the films was evaluated according to ASTM D3363 standard test method using Mitsubishi pencils with different hardness levels (4B~8H). Adhesion tests were conducted in accordance with ASTM D3359 cross-cut tape test by creating grids with 0.5 mm x 0.5 mm meshes using a cross-hatcher. Weakly adhesive 3M (Saint Paul, Minnesota, United States) scotch and strongly adhesive 3M VHB tapes were applied and peeled off vertically in a repeated manner (up to 10 times), and the grids were inspected for delamination under an optical microscope.